LETTER

doi:10.1038/nature22044

Antisense oligonucleotide therapy for spinocerebellar ataxia type 2

Daniel R. Scoles[1], Pratap Meera[2], Matthew D. Schneider[1], Sharan Paul[1], Warunee Dansithong[1], Karla P. Figueroa[1], Gene Hung[3], Frank Rigo[3], C. Frank Bennett[3], Thomas S. Otis[2]† & Stefan M. Pulst[1]

There are no disease-modifying treatments for adult human neurodegenerative diseases. Here we test RNA-targeted therapies[1] in two mouse models of spinocerebellar ataxia type 2 (SCA2), an autosomal dominant polyglutamine disease[2]. Both models recreate the progressive adult-onset dysfunction and degeneration of a neuronal network that are seen in patients, including decreased firing frequency of cerebellar Purkinje cells and a decline in motor function[3,4]. We developed a potential therapy directed at the *ATXN2* gene by screening 152 antisense oligonucleotides (ASOs). The most promising oligonucleotide, ASO7, downregulated *ATXN2* mRNA and protein, which resulted in delayed onset of the SCA2 phenotype. After delivery by intracerebroventricular injection to ATXN2-Q127 mice, ASO7 localized to Purkinje cells, reduced cerebellar *ATXN2* expression below 75% for more than 10 weeks without microglial activation, and reduced the levels of cerebellar ATXN2. Treatment of symptomatic mice with ASO7 improved motor function compared to saline-treated mice. ASO7 had a similar effect in the BAC-Q72 SCA2 mouse model, and in both mouse models it normalized protein levels of several SCA2-related proteins expressed in Purkinje cells, including Rgs8, Pcp2, Pcp4, Homer3, Cep76 and Fam107b. Notably, the firing frequency of Purkinje cells returned to normal even when treatment was initiated more than 12 weeks after the onset of the motor phenotype in BAC-Q72 mice. These findings support ASOs as a promising approach for treating some human neurodegenerative diseases.

SCA2 is caused by DNA CAG-repeat expansion leading to an increase in the polyglutamine (polyQ) domain in the N-terminal part of the ATXN2 protein. Although the disease was initially described as cerebellar degeneration, it is now known to involve multiple neuronal subtypes outside the cerebellum, and can also present as amyotrophic lateral sclerosis (ALS) or Parkinson disease[5,6]. Neurodegenerative diseases caused by dominant mutations in human genes have been difficult to approach therapeutically, and few studies have targeted disease genes directly as the first step in pathogenesis (discussed below). Developing therapeutics for SCAs can be complicated by the occurrence of repeat-associated non-AUG translation, which appears to be irrelevant for SCA2 (ref. 7). Although targeting the mutation itself appears attractive, this approach has proven to be technically difficult in polyQ diseases. We have used SCA2 as a model to develop an approach to use ASOs to directly target *ATXN2* mRNA.

ASOs have recently undergone substantial development[1]. Modification of DNA backbone chemistry has reduced toxicity, increased target engagement, and improved destruction of DNA–RNA hybrids. We designed multiple chimaeric 2′-*O*-methoxyethyl/DNA gapmer ASOs, which target *ATXN2*, for an *in vitro* screen and screened for *ATXN2* RNA reduction in a cell-based assay, identifying several ASOs that reduced *ATXN2* expression. After testing of these ASOs for *in vivo* tolerability, we tested one ASO in detailed behavioural, biochemical and physiological studies. This ASO targets exon 11 of human *ATXN2* and is designated ASO7.

In a previous study using mice that were homozygous for the polyQ-expanded ATXN2, a more severe disease manifestation was observed than in heterozygous littermate mice, indicating that ATXN2 dosage was important pathologically[8]. On the other hand, reducing *ATXN2* dosage did not affect survival or central nervous system morphology in heterozygous or homozygous knockout animals[9], suggesting *ATXN2* reduction by ASOs as a viable strategy for SCA2-mediated neurodegeneration.

Our *in vitro* screen included 152 ASOs designed *in silico* for targeting human *ATXN2*. The top 8 lead ASOs lowered *ATXN2* expression by $\geq$85% (Extended Data Fig. 1 and Supplementary Table 1). *In vivo* testing revealed ASO7 and two other ASOs among the most effective for lowering *ATXN2* expression after a seven day treatment (Extended Data Fig. 2a–c). To assess astroglial and microglial activation we measured cerebellar *Gfap* and *Aif1* expression by qPCR. We tested several doses of ASO7 and observed a significant reduction in *ATXN2* in cerebella after 14 days of treatment with 210 μg ASO7 without activation of *Gfap* or *Aif1* (Extended Data Figs 2a–c, 3). Some ASOs were not further pursued owing to activation of astroglial or microglial responses in treatments over 10 weeks. We verified that ASO7 as well as other lead ASOs were taken up by Purkinje cells by immunohistochemistry (Extended Data Fig. 2d–i).

ATXN2-Q127 mice have a human *ATXN2* cDNA transgene with 127 CAG repeats. We treated ATXN2-Q127 mice by intracerebroventricular injection (ICV) at 8 weeks of age, coinciding with the age of motor phenotype onset[4], with ASO7 and tested motor performance on the accelerating rotarod at weeks 5, 9 and 13 after ICV injection. Consensus criteria for the conduct of preclinical trials were closely followed (see Supplementary Discussion). Progression of motor dysfunction in saline-treated mice was as previously observed[4]. Mice injected with ASO7 had significantly improved motor performance compared to saline-treated control mice (Fig. 1a), and human *ATXN2* and mouse *Atxn2* mRNA levels were reduced by 75% and 20%, respectively, after motor phenotype testing, demonstrating target engagement (Fig. 2a–c).

In preclinical studies, it is important to test compounds in multiple models of the human disease. We therefore developed a mouse model that replicated the human disease more closely by expressing a bacterial-artificial-chromosome (BAC) transgene incorporating the human promoter as well as all exons, introns and flanking regions. The BAC resulted in expression of ATXN2 with 72 glutamines (Q72) in multiple neuronal tissues including the spinal cord[3]. The BAC-Q72 model approximates human disease not only with regard to disease manifestation and less pronounced progression, but also because it contains the entire human gene in its proper intronic–exonic context. We conducted an additional preclinical trial in this mouse model with

[1]Department of Neurology, University of Utah, 175 North Medical Drive East, 5th Floor, Salt Lake City, Utah 84132, USA. [2]Department of Neurobiology, University of California Los Angeles, Los Angeles, California 90095, USA. [3]Ionis Pharmaceuticals, 2855 Gazelle Court, Carlsbad, California 92010, USA. †Present address: Roche Pharma Research and Early Development, Neuroscience, Ophthalmology & Rare Diseases, Roche Innovation Center Basel, Grenzacherstrasse 124, CH-4070 Basel, Switzerland.

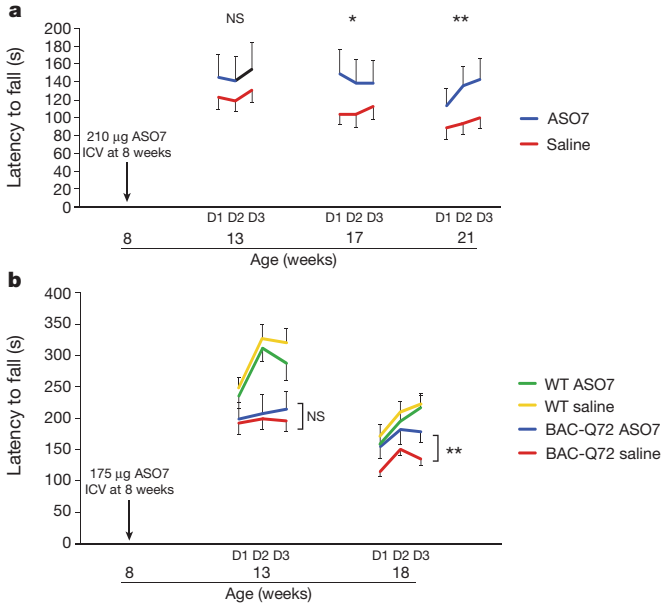

Figure 1 | Effect of ASO7 on motor phenotypes. a, Eight-week-old ATXN2-Q127 mice were treated with 210 μg ASO7 or saline ICV and tested on the rotarod at the indicated ages. $n = 15$ mice per group. **b**, Eight-week-old BAC-Q72 mice and wild-type (WT) littermates were treated with 175 μg ASO7 or saline ICV and tested on the rotarod at the indicated ages. $n = 13$ and 13, for wild-type mice treated with ASO7 and saline, respectively; $n = 11$ and 14, for BAC-Q72 mice treated with ASO7 and saline, respectively. Values are mean ± s.e.m. Probabilities of significance were determined using the method of generalized estimating equations. $^*P < 0.05$; $^{**}P < 0.01$; NS, not significant.

treatment that was initiated at 8 weeks of age, as for the experiment using ATXN2-Q127 mice. Again, the mutated human *ATXN2* and mouse *Atxn2* were engaged by ASO7 with mRNA levels that were reduced by 60% and 26%, respectively (Fig. 2d), and human ATXN2 was not detected in cerebellar lysates from treated mice by western blotting (Fig. 2e, f). Ten weeks after ICV injection, significant improvement in motor behaviour was seen in ASO7-treated mice compared to saline-injected mice (Fig. 1b). However, the rotarod performance of the ASO7-treated mice did not perfectly mirror that of wild-type mice. This might indicate that additional treatment time would be necessary to more completely restore cerebellar function. Rotarod results observed were not affected by differences in mouse weights between the experimental groups (Extended Data Fig. 4).

Previously, we established transcriptome and protein profiles characterized by progressive changes in the course of degeneration in SCA2 mouse models[3]. To evaluate the effect of ASO7 on steady-state mRNA and protein levels we chose the top 6 mRNAs that showed the most significant changes in both mouse models[3]. Given that the ATXN2-Q127 model expresses the transgene specifically in Purkinje cells, we investigated genes significantly altered by SCA2 progression that are highly and specifically expressed in Purkinje cells: *Rgs8*, *Pcp2*, *Pcp4*, *Cep76*, *Homer3* and *Fam107b* (ref. 3). RGS proteins inhibit mGlur1 (ref. 10), which is a positive regulator of Ca^{2+} release from internal stores[11]. Because mGlur1 signalling is disrupted in SCA2 Purkinje cells leading to abnormal Ca^{2+} release, mGlur1 regulation may also be a function of Rgs8 (refs 3,12). mGlur1 is also regulated in Purkinje cells by Homer3 (ref. 13). Pcp2 is a regulator of $G_{i/o}$-coupled receptors including the P-type Ca^{2+} channel, which is important for sensorimotor control[14]. Loss of Pcp4 causes abnormal parallel fibre synapses in Purkinje cells[15], and Cep76 is required for normal centriole function[16]. *Fam107b* and *Rgs8* were identified as cerebellar hub genes

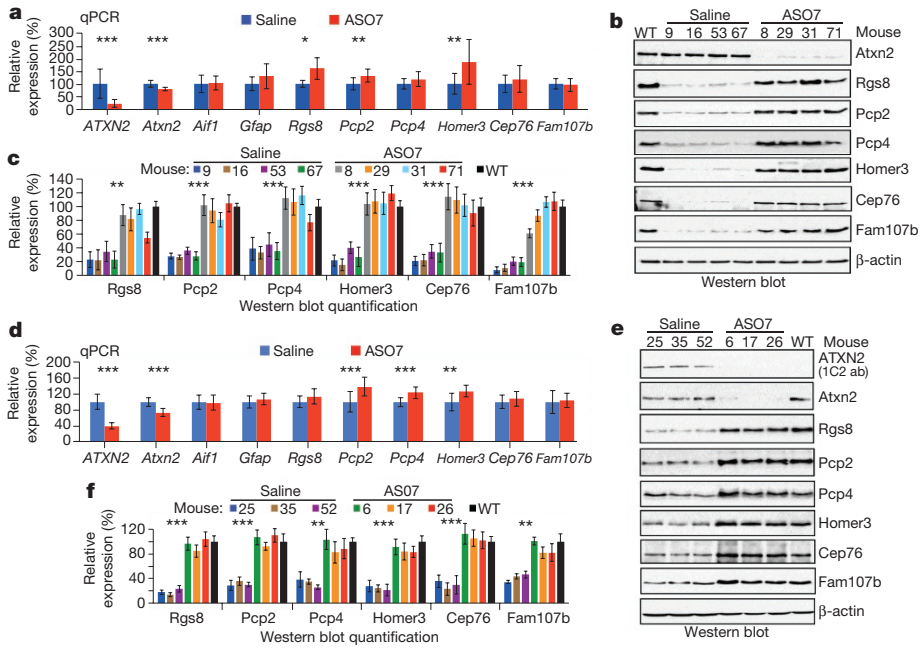

Figure 2 | Cerebellar gene expression for ASO7-treated SCA2 mice following rotatod tests. a–c, Expression in ATXN2-Q127 mice. **a**, ATXN2-Q127 mice were treated as in Fig. 1a and the cerebellar expression of the indicated genes was determined by qPCR relative to *Actb* at 22 weeks of age. The number of mice for saline and ASO7 treatments, respectively, were: *ATXN2*, 11 and 11; *Atxn2*, 11 and 11; *Aif1*, 7 and 8; *Gfap*, 11 and 11; *Rgs8*, 4 and 4; *Pcp2*, 11 and 11; *Pcp4*, 10 and 11; *Cep76*, 10 and 11; *Homer3*, 10 and 11; *Fam107b*, 10 and 10 mice. **b**, **c**, Cerebellar expression in ATXN2-Q127 mice for ATXN2, mouse Atxn2, Rgs8, Pcp2, Pcp4, Cep76, Homer3, Fam107b and β-actin (**b**), with abundances expressed relative to β-actin, determined by densitometry (**c**). Numbers indicate mouse identifiers. **d**–**f**, Expression in BAC-Q72 mice. **d**, BAC-Q72 mice were treated as in Fig. 1b and the cerebellar expression of the indicated genes was determined at 19 weeks of age. The number of mice per group in qPCR analyses was 14 saline-treated mice and 11 ASO7-treated mice for all genes except *Rgs8* and *Fam107b*, where the *n* was 14 saline-treated and 10 ASO-treated mice. **e**, Cerebellar expression in BAC-Q72 mice of expanded ATXN2 detected with anti-1C2 antibody, and expression of mouse Atxn2, Rgs8, Pcp2, Pcp4, Cep76, Homer3, Fam107b and β-actin (**e**), with abundances expressed relative to β-actin, determined by densitometry (**f**). Values are mean ± s.d. from the number of mice indicated (**a**, **d**) or from three replicate blots (**c**, **f**). $^*P < 0.05$; $^{**}P < 0.01$; $^{***}P < 0.001$; NS, not significant; by Student's *t*-test.

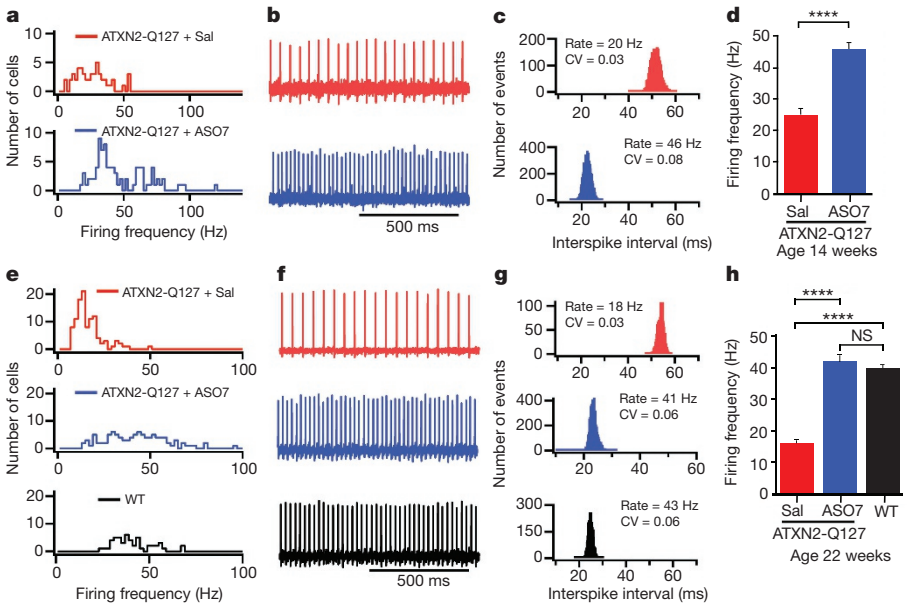

Figure 3 | Slow firing frequency of Purkinje cells from ATXN2-Q127 mice was restored by ASO7. a–d, ATXN2-Q127 mice were treated with 210 μg ASO7 or saline by ICV injection at 8 weeks, and the firing frequency of Purkinje cells was evaluated at 14 weeks of age. Sal, saline. **a**, Mean distribution of firing frequencies for Purkinje cells from saline- and ASO7-treated mice. **b**, **c**, Representative traces of 1 s duration from Purkinje cells (**b**) and interspike-interval histogram (**c**) of the same cell as in **b**, calculated for a 2 min duration, with coefficients of variation (CV) shown. **d**, The firing frequencies (mean ± s.e.m.) were 25 ± 2 Hz for the saline-treated mouse ($n = 50$ neurons, $n = 1$ mouse) and 46 ± 2 Hz for ASO7-treated mice ($n = 88$ neurons, $n = 2$ mice). **e–h**, ATXN2-Q127 mice were treated with 210 μg ASO7 or saline by ICV injection at 8 weeks. The firing frequency of Purkinje cells was evaluated at 22 weeks of age. **e**, Mean firing frequencies of all Purkinje cells measured from saline- and ASO7-treated mice and age-matched wild-type mice. **f**, **g**, Representative traces of 1 s duration of Purkinje cells (**f**) and interspike-interval histogram (**g**) of the same cell as in **f**, calculated for a 2 min duration, with values for the coefficient of variation shown. **h**, The firing frequencies (mean ± s.e.m.) were 16 ± 1 Hz for saline-treated ATXN2-Q127 mice ($n = 107$ neurons, $n = 2$ mice), 42 ± 2 Hz for the ASO7-treated ATXN2-Q127 mice ($n = 102$ neurons, $n = 2$ mice), and 40 ± 1 Hz for an age-matched wild-type mouse ($n = 50$ neurons, $n = 1$ mouse). All recordings were measured at 34.5 ± 1 °C. $****P < 0.0001$, Student's *t*-test.

with reduced expression in SCA1 mice[17]. Although significant increases at the mRNA level occurred for half of the genes after ASO7 treatment (Fig. 2), we observed restored protein expression for all six of the genes on western blots (Fig. 2, uncropped western blots in Supplementary Fig. 1). This observation is consistent with an emerging role of polyglutamine-expanded ATXN2 in translational dysregulation[3,18].

Purkinje cells are neurons that fire spontaneously with a resting firing frequency of 40–50 Hz in mammals. The circuits that underlie cerebellar learning and functioning are well understood[12,19,20], whereby the Purkinje cells integrate signals received from parallel and climbing fibres and provide the only output from cerebellar cortex to deep cerebellar nuclei. In acute slice preparations, we have previously shown that mutant *ATXN2* caused a slowing of Purkinje cell firing. This change had an onset and progression that closely mirrored that of motor deficits with onset at 6–8 weeks and the firing rate eventual slowed to 20 Hz at 24 weeks of age[4]. It has been suggested that the change in the physiology of Purkinje cells is tightly linked to Ca^{2+} homeostasis and subsequent cell death[12,21]. This tight linkage between behaviour and physiology led us to hypothesize that ASO treatment would restore normal Purkinje cell firing. We injected ATXN2-Q127 mice at 8 weeks and analysed Purkinje cell physiology 6 and 14 weeks later in acute cerebellar slices. Similarly, we injected BAC-Q72 mice at 30 weeks, over 12 weeks after motor phenotype onset, and analysed Purkinje cell firing 10 weeks later. In both models, a single injection of ASO7 resulted in near complete restoration of normal Purkinje cell firing frequency (Figs 3, 4). The mice used in these experiments were subsets of those in Fig. 1a, b, and had established rotarod phenotypes. These results suggest that *ATXN2* ASO treatment directly affects Purkinje cell physiology and at least in part explains the amelioration of motor behaviour.

SCA2 and other polyglutamine diseases are characterized by toxic gains of function, suggesting that therapeutics that lower the expression of the disease-causing genes would be beneficial. ASOs represent an ideal approach for directly lowering *ATXN2* expression, because ASOs are sequence-specific, well-tolerated, and can reach central nervous system targets by intrathecal delivery. Feasibility is further supported by an early-phase human clinical trial to develop an ASO therapy for SOD1-ALS[22], and most recently by the FDA approval of the ASO drug nusinersin for spinal muscular atrophy. Various approaches to ASO therapeutics for polyglutamine diseases have been developed including targeting wild-type and mutant alleles as in this study or attempting to target mutant alleles through the expanded CAG repeat or through single nucleotide polymorphisms that are in linkage disequilibrium with the mutation[23,24]. Deep cerebellar nuclei that were injected with adeno-associated viruses, which targeted shRNAs to Purkinje cells, were also effective for SCA1, reducing target expression and improving motor and cerebellar phenotypes in SCA1-transgenic mice[25,26]. At least for SCA2 and with the caveats of preclinical mouse studies, the strategy of targeting both mutant and wild-type alleles is showing promise. One potential advantage of ASOs over current viral vectors is that they distribute through the nervous system, whereas adenoviral vectors are primarily transported transynaptically (also, gene transfer comes with more complex safety concerns). Therefore, for SCA2, adeno-associated viruses that are injected into neurons from the deep cerebellar nuclei would reach Purkinje cells, but may not reach other neuronal groups.

In conclusion, we rigorously screened ASOs to identify a potent and well-tolerated ASO, ASO7, that lowered cerebellar *ATXN2* expression, and verified in two SCA2 models that ASO7 delayed SCA2 motor and electrophysiological phenotypes in replicate experiments. Cerebellar degenerative diseases provide excellent model systems to study the interaction of dysfunction in a neuronal network, behaviour and neurodegeneration. Our study suggests that reduction of mutant ATXN2 affects all three domains including endophenotypic markers of cell death common in ataxias[3,17,27]. Multiple lines of evidence suggest

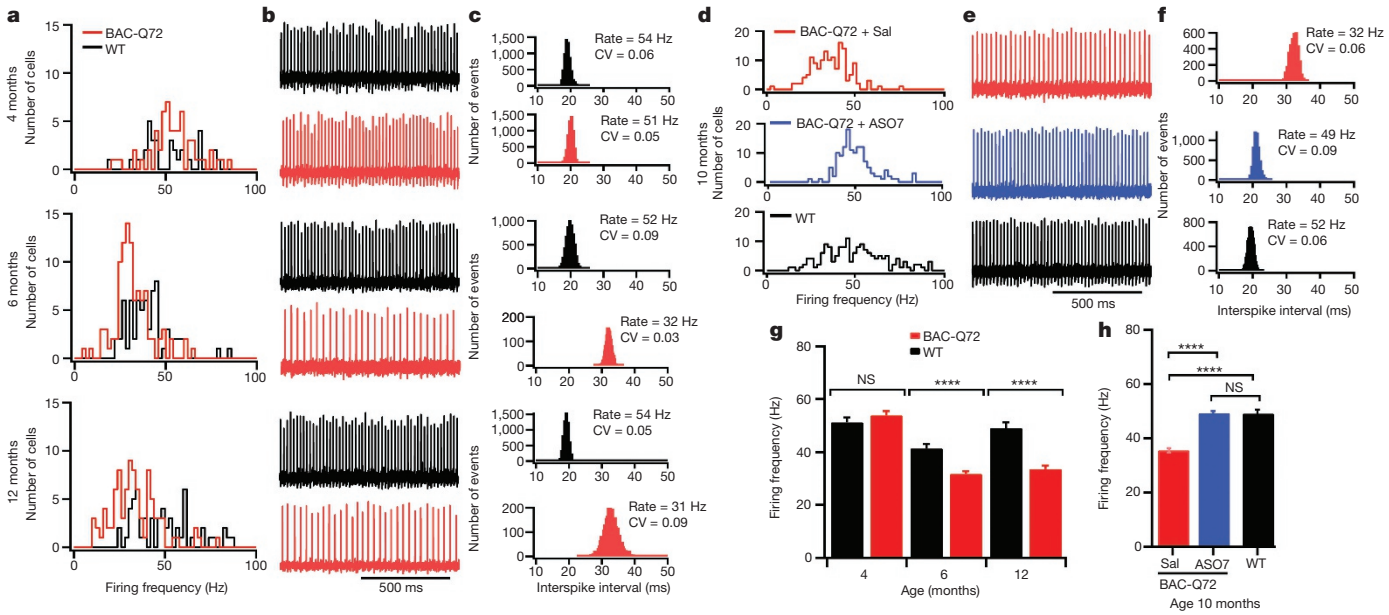

Figure 4 | Slow firing frequency of Purkinje cells from BAC-Q72 mice was restored by ASO7. a–**c**, Firing frequencies of BAC-Q72 mice at the indicated ages. **a**, Distributions of the firing frequency for wild-type and BAC-Q72 Purkinje cells. The number of Purkinje cells were (the age of mice is indicated in brackets): $n = 33$ wild-type and 59 BAC-Q72 (4 months); 49 wild-type and 101 BAC-Q72 (6 months); 55 wild-type and 92 BAC-Q72 (12 months) cells. **b**, Example recordings from Purkinje cells for wild-type and BAC-Q72 mice. **c**, Interspike intervals of the same cell over 2 min with mean firing frequency and coefficients of variation indicated. **d**–**f**, The firing frequency of Purkinje cells was restored in ten-month-old BAC-Q72 mice treated with 210 μg ASO7 for 10 weeks. **d**, The firing frequency of Purkinje cells in BAC-Q72 mice, BAC-Q72 mice treated with ASO7 and wild-type littermates. **e**, **f**, Representative 1-s trace of Purkinje cells (**e**) and interspike intervals (**f**) of the same cells over 2 min in saline-treated BAC-Q72 mice, ASO-treated BAC-Q72 and wild-type littermates with Purkinje cell firing frequency and coefficients of variation indicated. **g**, **h**, Mean firing frequency of Purkinje cells in **a** and **d**. **g**, Age-dependent firing frequency of Purkinje cells from BAC-Q72 mice. At 4 months the mean firing frequencies in Hz were 51 ± 2 for wild-type ($n = 33$ Purkinje cells, $n = 1$ mouse) and 54 ± 2 for BAC-Q72 ($n = 59$ Purkinje cells, $n = 1$ mouse). At 6 months the values were 41 ± 2 Hz for wild-type ($n = 49$ Purkinje cells, $n = 2$ mice) and 32 ± 1 Hz for BAC-Q72 ($n = 101$ Purkinje cells, $n = 2$ mice). At 12 months, values were 49 ± 2 Hz for wild-type ($n = 55$ Purkinje cells, $n = 1$ mouse) and 34 ± 1 for BAC-Q72 ($n = 92$ Purkinje cells, $n = 1$ mouse). **h**, ASO7 treatment restored the firing frequency of Purkinje cells from BAC-Q72 mice. The mean firing frequency of Purkinje cells from ten-month-old BAC-Q72 mice treated with saline was 36 ± 1 Hz ($n = 148$ Purkinje cells, $n = 3$ mice), whereas the mean firing frequency of BAC-Q72 mice treated with ASO7 was 49 ± 1 Hz ($n = 134$ Purkinje cells, $n = 4$ mice), similar to that of wild-type mice (49 ± 1 Hz, $n = 155$ Purkinje cells, $n = 3$ mice). $^{****}P < 0.0001$, ANOVA followed by Tukey's multiple-comparison post hoc testing.

that ASOs may have applications in human patients. ASO7 lowered expression of wild-type and mutant ATXN2 in SCA2 patient-derived fibroblasts (Extended Data Fig. 5). ASO7 delivered by ICV injection localized throughout the spinal column and lowered *ATXN2* expression not only in brain, but also in spinal cord (data not shown). Notably, lowering of ATXN2 by ASO treatment or genetic knockout delays dysfunction and greatly extends survival of *TDP-43* transgenic ALS mice.[28]. ASO7 or ASOs with further modifications in ASO chemistry may provide an effective human drug for SCA2, ALS caused by *ATXN2* mutation and other forms of ALS.

Online Content Methods, along with any additional Extended Data display items and Source Data, are available in the online version of the paper; references unique to these sections appear only in the online paper.

Received 24 June 2016; accepted 6 March 2017.
Published online 12 April 2017.

1. Rigo, F., Seth, P. P. & Bennett, C. F. Antisense oligonucleotide-based therapies for diseases caused by pre-mRNA processing defects. *Adv. Exp. Med. Biol.* **825,** 303–352 (2014).
2. Pulst, S. M., Nechiporuk, A. & Starkman, S. Anticipation in spinocerebellar ataxia type 2. *Nat. Genet.* **5,** 8–10 (1993).
3. Dansithong, W. *et al.* Ataxin-2 regulates RGS8 translation in a new BAC-SCA2 transgenic mouse model. *PLoS Genet.* **11,** e1005182 (2015).
4. Hansen, S. T., Meera, P., Otis, T. S. & Pulst, S. M. Changes in Purkinje cell firing and gene expression precede behavioral pathology in a mouse model of SCA2. *Hum. Mol. Genet.* **22,** 271–283 (2013).
5. Pulst, S. M. Degenerative ataxias, from genes to therapies: The 2015 Cotzias Lecture. *Neurology* **86,** 2284–2290 (2016).
6. Houlden, H. & Singleton, A. B. The genetics and neuropathology of Parkinson's disease. *Acta Neuropathol.* **124,** 325–338 (2012).
7. Scoles, D. R. *et al.* Repeat associated non-AUG translation (RAN translation) dependent on sequence downstream of the ATXN2 CAG repeat. *PLoS One* **10,** e0128769 (2015).
8. Huynh, D. P., Figueroa, K., Hoang, N. & Pulst, S. M. Nuclear localization or inclusion body formation of ataxin-2 are not necessary for SCA2 pathogenesis in mouse or human. *Nat. Genet.* **26,** 44–50 (2000).
9. Huynh, D. P., Maalouf, M., Silva, A. J., Schweizer, F. E. & Pulst, S. M. Dissociated fear and spatial learning in mice with deficiency of ataxin-2. *PLoS One* **4,** e6235 (2009).
10. Saugstad, J. A., Marino, M. J., Folk, J. A., Hepler, J. R. & Conn, P. J. RGS4 inhibits signaling by group I metabotropic glutamate receptors. *J. Neurosci.* **18,** 905–913 (1998).
11. Abdul-Ghani, M. A., Valiante, T. A., Carlen, P. L. & Pennefather, P. S. Metabotropic glutamate receptors coupled to IP3 production mediate inhibition of IAHP in rat dentate granule neurons. *J. Neurophysiol.* **76,** 2691–2700 (1996).
12. Meera, P., Pulst, S. M. & Otis, T. S. Cellular and circuit mechanisms underlying spinocerebellar ataxias. *J. Physiol. (Lond.)* **594,** 4653–4660 (2016).
13. Mizutani, A., Kuroda, Y., Futatsugi, A., Furuichi, T. & Mikoshiba, K. Phosphorylation of Homer3 by calcium/calmodulin-dependent kinase II regulates a coupling state of its target molecules in Purkinje cells. *J. Neurosci.* **28,** 5369–5382 (2008).
14. Iscru, E. *et al.* Sensorimotor enhancement in mouse mutants lacking the Purkinje cell-specific $G_{i/o}$ modulator, Pcp2(L7). *Mol. Cell. Neurosci.* **40,** 62–75 (2009).
15. Wei, P., Blundon, J. A., Rong, Y., Zakharenko, S. S. & Morgan, J. I. Impaired locomotor learning and altered cerebellar synaptic plasticity in *pep-19/PCP4*-null mice. *Mol. Cell. Biol.* **31,** 2838–2844 (2011).
16. Tsang, W. Y. *et al.* Cep76, a centrosomal protein that specifically restrains centriole reduplication. *Dev. Cell* **16,** 649–660 (2009).
17. Ingram, M. *et al.* Cerebellar transcriptome profiles of ATXN1 transgenic mice reveal SCA1 disease progression and protection pathways. *Neuron* **89,** 1194–1207 (2016).
18. Fittschen, M. *et al.* Genetic ablation of ataxin-2 increases several global translation factors in their transcript abundance but decreases translation rate. *Neurogenetics* **16,** 181–192 (2015).

19. Lee, K. H. *et al.* Circuit mechanisms underlying motor memory formation in the cerebellum. *Neuron* **86,** 529–540 (2015).
20. Lang, E. J. *et al.* The roles of the olivocerebellar pathway in motor learning and motor control. A consensus paper. *Cerebellum* **16,** 230–252 (2017).
21. Liu, J. *et al.* Deranged calcium signaling and neurodegeneration in spinocerebellar ataxia type 2. *J. Neurosci.* **29,** 9148–9162 (2009).
22. Miller, T. M. *et al.* An antisense oligonucleotide against SOD1 delivered intrathecally for patients with SOD1 familial amyotrophic lateral sclerosis: a phase 1, randomised, first-in-man study. *Lancet Neurol.* **12,** 435–442 (2013).
23. Skotte, N. H. *et al.* Allele-specific suppression of mutant huntingtin using antisense oligonucleotides: providing a therapeutic option for all Huntington disease patients. *PLoS One* **9,** e107434 (2014).
24. Carroll, J. B. *et al.* Potent and selective antisense oligonucleotides targeting single-nucleotide polymorphisms in the Huntington disease gene/allele-specific silencing of mutant huntingtin. *Mol. Ther.* **19,** 2178–2185 (2011).
25. Xia, H. *et al.* RNAi suppresses polyglutamine-induced neurodegeneration in a model of spinocerebellar ataxia. *Nat. Med.* **10,** 816–820 (2004).
26. Keiser, M. S., Boudreau, R. L. & Davidson, B. L. Broad therapeutic benefit after RNAi Expression vector delivery to deep cerebellar nuclei: implications for spinocerebellar ataxia type 1 therapy. *Mol. Ther.* **22,** 588–595 (2014).
27. Rodriguez-Lebron, E., Liu, G., Keiser, M., Behlke, M. A. & Davidson, B. L. Altered Purkinje cell miRNA expression and SCA1 pathogenesis. *Neurobiol. Dis.* **54,** 456–463 (2013).
28. Becker, L. A. *et al.* Therapeutic reduction of ataxin-2 extends lifespan and reduces pathology in TDP-43 mice. *Nature* http://dx.doi.org/10.1038/nature22038 (2017).

Supplementary Information is available in the online version of the paper.

Acknowledgements We thank P. Jafar-Nejad for his contributions to interpreting results and for reading and editing the manuscript, L. Pflieger for contributing to the production of Supplementary Data. This work was supported by grants R01NS33123, R56NS33123 and R37NS033123 from the National Institutes of Neurological Disorders and Stroke (NINDS) to S.M.P., the Noorda foundation to S.M.P., NINDS grants RC4NS073009 and R21NS081182 to D.R.S. and S.M.P., NINDS grant NS090930 to T.S.O., and a gift from Ionis Pharmaceuticals. S.M.P. received grant support from the Target ALS Foundation.

Author Contributions D.R.S. conceived and designed the study, performed experiments, conducted all ICV injections, analysed all data and wrote the manuscript. M.S. performed all motor-testing experiments and with D.R.S. contributed to blinding of all mouse trials including ASO treatments, motor testing and electrophysiological evaluations. M.D.S. also conducted all qPCR analyses of mouse tissues. P.M. designed and performed all electrophysiological experiments, analysed and interpreted the resulting data, and prepared figures. S.P. prepared all western blots. W.D. conducted the study of SCA2 patient-derived fibroblasts. K.P.F. was in charge of mouse breeding. G.H. led the ASO *in silico* design, ASO *in vitro* screening, advised the *in vivo* screening approach, and provided ASOs. F.R. and C.F.B. contributed to the *in vivo* screening approach, design of motor phenotype studies, and interpretation of results. T.S.O. designed and helped interpret the electrophysiological analyses. S.M.P. conceived and designed the study with D.R.S. and contributed SCA2 patient-derived fibroblasts. All authors contributed to the writing of the manuscript.

Author Information Reprints and permissions information is available at www.nature.com/reprints. The authors declare competing financial interests: details are available in the online version of the paper. Readers are welcome to comment on the online version of the paper. Publisher's note: Springer Nature remains neutral with regard to jurisdictional claims in published maps and institutional affiliations. Correspondence and requests for materials should be addressed to D.R.S. (Daniel.Scoles@hsc.utah.edu) or S.M.P. (Stefan.Pulst@hsc.utah.edu).

Reviewer Information *Nature* thanks R. L. Juliano, J. Rothstein and T. Siddique for their contribution to the peer review of this work.

METHODS

SCA2 mice. *Pcp2-ATXN2*-Q127 (ATXN2-Q127) transgenic mice express the full-length human *ATXN2*-$(CAG)_{127}$ cDNA under the control of the mouse Purkinje cell protein 2 (L7) promoter (*Pcp2*). ATXN2-Q127 mice in this study had a C57BL/6J;DBA/2J (B6;D2) hybrid background. ATXN2-Q127 mice are described in refs 3,4. BAC-ATXN2-Q72 (BAC-Q72) mice were created using a contiguous 169 kb human *ATXN2* gene sequence including 16 kb upstream *ATXN2* sequence, the entire *ATXN2*-$(CAG)_{72}$ coding region (with introns) and 3 kb of *ATXN2* 3′-UTR and downstream sequence. BAC-Q22 mice are identical to BAC-Q72 mice, but with the normal length CAG repeat. BAC-Q22 and BAC-Q72 mice used in this study had a FVB;C57BL/6 hybrid background. The generation of the BAC-Q72 and BAC-Q22 mice is described in ref. 3. BAC-Q22 mice were used in some *in vivo* ASO testing experiments that are not shown. Animals were genotyped by two separate PCR reactions using SCA2A/SCA2B and BM13-F/BM14-R genotyping primers (Supplementary Table 2). One week after surgery animals were recombined into cages of four mice for the duration of the study. Mouse groups included a balance of males and females. All animal work was done with approved IACUC protocols at the University of Utah and University of California Los Angeles.

All mouse treatment trials were blinded to the tester. Randomized mouse groups for rotarod tests were arranged by a technician and rotarod testing performed by a second technician not aware of group assignment of mouse genotype. To ensure blinding, ASO-treated and saline-treated mice were housed together and the technician performing behavioural testing was not aware of treatment status. Group assignments were not identifiable by the technician performing phenotype evaluations. For rotarod testing, rotarod groups were controlled for baseline rotarod performance as well as weight. Additionally, when mice were transported to the neurophysiology laboratory they were encoded such that ASO treatments were blinded to the investigator performing electrophysiology testing. We also blinded the technician performing qPCR analyses using mice post phenotype testing. These measures ensured that all determinations of the effects of ASO treatments on SCA2 mice were made in an unbiased, operator-independent manner. Additional comments on study rigor including blinding are provided in the Supplementary Discussion.

Antisense oligonucleotides. All antisense oligonucleotides were 20 bp in length, included five 2′-*O*-methoxyethyl-modified nucleotides at each end of the oligonucleotide, with ten DNA nucleotides in the centre, and were phosphorothioate modified in all positions. ASOs were synthesized as previously described[29]. The program Bowtie[30] was used to determine the predicted off-targets for the *ATXN2* ASOs in the mouse transcriptome (preRNA and mRNA). This analysis confirmed that the *ATXN2* ASOs do not bind any RNA other than *ATXN2* with full complementarity. We further verified that none of the lead ASOs had sequences that would target the closely homologous *ATXN2L* gene.

ICV ASO injections. ASOs were delivered to mice by intracerebroventricular (ICV) injection. Injection were carried out using a Hamilton 26-s gauge needle. For mice in Figs 1–4, injections were 6 μl of 35 μg μl^{-1} ASO7 diluted in normal saline for a total of 210 μg. Control mice received the same volume of normal saline. For other mice in the Extended Data Figs, injection volumes varied from 6–10 μl to deliver the indicated ASO concentrations, with ASOs diluted accordingly with normal saline. Injections were made under anaesthesia with a mixture of oxygen and isoflurane, using a Stoelting stereotaxic frame. Anaesthesia was initiated using 3% isoflurane for 5 min and the isoflurane mixture was lowered to 2% during injections. Stereotaxic bregma coordinates were −0.46 mm anteroposterior, −1.0 mm lateral (right side) and −2.5 mm dorsoventral. Needles were removed 4 min after ASO delivery. Mice were maintained on a 39 °C isothermal pad while anaesthetized and during recovery.

Cell culture. SCA2 patient-derived skin fibroblasts (SCA2(CAG35)) were cultured and maintained in DMEM medium supplemented with 10% fetal bovine serum, penicillin and streptomycin. All subjects gave written consent and the studies were approved by the Institutional Review Board at the University of Utah. ASO transfections were performed by electroporation of one million cells with 0, 0.35, 1 or 2 μM ASO7 using the Neon transfection system (Invitrogen) according to the manufacturer's protocol, followed by plating in 6-well plates. The cells were collected five days after electroporation for analyses.

Western blot analyses. Protein extracts were prepared by homogenization of mouse cerebella in extraction buffer (25 mM Tris-HCl pH 7.6, 300 mM NaCl, 0.5% Nonidet P-40, 2 mM EDTA, 2 mM $MgCl_2$, 0.5 M urea and protease inhibitors; Sigma; P-8340) followed by centrifugation at 4 °C for 20 min at 16,100*g*. Only supernatants were used for western blotting to determine the steady-state levels of proteins using the antibodies listed below. Protein extracts were resolved by SDS–PAGE and transferred to Hybond P membranes (Amersham Bioscience). After blocking with 5% skim milk in 0.1% Tween 20/PBS, the membranes were incubated with primary antibodies in 5% skim milk in 0.1% Tween 20/PBS for 2 h at room temperature or overnight at 4 °C. After washing in 0.1% Tween 20/PBS, the membranes were incubated with the corresponding secondary antibodies conjugated with HRP in 5% skim milk in 0.1% Tween 20/PBS for 2 h at room temperature and washed again. Signals were detected by the Immobilon Western Chemiluminescent HRP Substrate (Millipore, WBKLSO100) according to the manufacturer's protocol. The intensity of proteins was determined using the ImageJ software analysis system and proteins were quantitated as a ratio to β-actin.

Immunohistochemical staining. Excised tissues were fixed in 4% paraformaldehyde for 72 h, and were then treated in 75% ethanol for 24 h, after which paraffin embedding was performed by automated instrumentation (University of Utah Histology Core). Embedded tissues were sectioned in 4-μm sections on a Leica microtome and mounted on glass slides. Sections were then deparaffinized and rehydrated (two washes in xylene, two washes in 100% ethanol, two washes in 95% ethanol, one wash in water). Endogenous peroxidases were quenched by treating in 3% H_2O_2 in methanol for 10 min followed by two washes in 1× wash buffer (TA-999-TT, Fisher Scientific). Sections were treated with Proteinase K for 10 min (Dako, S3020) then washed twice. Sections were treated with Cyto-Q Background Buster (Innovex Biosciences) then washed twice. Primary rabbit anti-ASO antibody (Ionis Pharmaceuticals) diluted 1:40,000 in antibody diluent (2% BSA, 5% normal donkey serum, in 1× wash buffer) was then incubated on sections overnight at 4 °C. Sections were then washed three times and incubated in secondary donkey anti-rabbit-HRP antibody (Jackson ImmunoResearch) 1:200 in antibody diluent for 30 min at room temperature, followed by three washes in wash buffer. Antibody detection was accomplished using DAB Chromagen (DAKO) followed by two washes in wash buffer. Sections were counterstained using haematoxylin (Fisher), washed twice in water, dipped in an acid–ethanol decolorizing solution (500 μl HCl to 200 ml of 70% ethanol), and washed in water. Sections were then dehydrated (two washes in 95% ethanol, two washes in 100% ethanol, two washes in xylene) and mounted using permamount (Fisher). Peroxidase staining was imaged on an EVOS FL Microscope using 2×, 10× and 40× objectives.

Antibodies. The following antibodies were used for western blotting: ATXN2 mAb (1: 4,000) (BD Biosciences, 611378), 5TF1-1C2 mAb (1:3,000) (Millipore, MAB1574), RGS8 rabbit polyclonal Ab (1:5,000) (Novus Biologicals, NBP2-20153), PCP2 antibody (F-3) (1: 3,000) (Santa Cruz, sc-137064), β-Actin mAb HRP conjugated (1:10,000) (Sigma-Aldrich, A3854). Anti-PCP4 antibody (1: 5,000) (Abcam, ab197377), Homer-3 antibody (E-6) (1: 2,000) (Santa Cruz, sc-376155), CEP76 antibody (1: 5,000) (Novus Biologicals, NBP1-28749), Anti-FAM107B antibody (1: 5,000) (Abcam, ab175148). The secondary antibodies were goat anti-mouse IgG-HRP antibody (1:5,000) (Sigma-Aldrich, A2304) and goat anti-rabbit IgG-HRP antibody (1:5,000) (Vector laboratories, PI-1000). Anti-ASO antibody (Ionis Pharmaceuticals) and appropriate secondary antibody used for immunohistochemistry are described in the previous paragraph.

Quantitative PCR. Total RNA was extracted from cerebellar tissues, spinal cord tissues or SCA2(CAG35) patient-derived fibroblasts using the RNeasyMini Kit (Qiagen) according to the manufacturer's protocol. DNase-I-treated RNAs were used to synthesize cDNAs using the ProtoScript cDNA First Strand cDNA Synthesis Kit (New England Biolabs). Primers for quantitative real-time PCR were designed to prevent amplification from genomic DNA (annealing sites in different exons or across intron–exon boundaries). PCR primers sequences are provided in Supplementary Table 2. Quantitative RT–PCR was performed in Bio-Rad CFX96 (Bio-Rad) with the Power SYBR Green PCRMasterMix (Applied Biosystems). PCR reaction mixtures contained SYBR Green PCRMasterMix and 0.5 pmol primers and PCR amplification was carried out for 45 cycles: denaturation at 95 °C for 10 s, annealing at 60 °C for 10 s and extension at 72 °C for 40 s. The threshold cycle for each sample was chosen from the linear range and converted to a starting quantity by interpolation from a standard curve run on the same plate for each set of primers. Gene expression levels were normalized to the mRNA levels for *Actb* (for mouse tissues) or *GAPDH* (for patient-derived fibroblasts).

Rotarod testing. Cohorts of mice were bred from randomly selected breeding animals. Cohorts were selected randomly to have a balanced number of males and females. Rotarod groups were controlled for baseline rotarod performance as well as weight (treatment groups within any experiment had the same average rotarod latency to fall and weight before treatments). Rotarod testing was performed on the Rotamex-5 instrument (Columbus Instruments). When performing tests, animals were taken to a separate testing room and habituated there for at least an hour before testing. Animals were tested in the same order, and beginning at the same time each day (13:00). Mice in different treatment groups were housed together and the technician was blinded to treatment status. All rotarod testing in this study was performed by the same technician. Rotarod values per each week of testing were collected over five days. On day 1 mice were handled for 2 min per mouse. On day 2 mice were introduced to the rotarod using the following paradigm: 4 r.p.m. for 2 min, then increasing by 1 r.p.m. per every 15 s to 10 r.p.m. for 60 s. Tests on days 3–5 on the accelerating rotarod were identical with three tests per day as follows:

mice were placed on the rod, which from 0 r.p.m. accelerated 1 r.p.m. every 9 s until mice fell from the rod. Most mice fell before 40 r.p.m. (6 min); all mice fell before 50 r.p.m. (7.5 min). Values of latency to fall in seconds were recorded. The rotarod was cleaned between individual tests. No animals were disqualified from testing once testing had begun, either during training or testing phases. Note that the *n* mice per group used in rotarod tests of 11–15 equals or exceeds the minimal *n* of 11 indicated by power analyses needed to maintain >80 % power to detect significant differences between groups with effect size >50% in a typical repeated-measures ANOVA.

Electrophysiology. The preparation of parasagittal cerebellar slices closely followed our previously published description of the process[31]. Cerebella from BAC-Q72, ATXN2-Q127 and their age-matched wild-type littermates were removed and quickly immersed in 4 °C extracellular solution bubbled with 95% O_2 and 5% CO_2 (119 mM NaCl, 26 mM $NaHCO_3$, 11 mM glucose, 2.5 mM KCl, 2.5 mM $CaCl_2$, 1.3 $MgCl_2$ and 1 mM NaH_2PO_4, pH 7.4 when gassed with 5% CO_2/95% O_2). Parasagittal cerebellar slices (285 μm) were sectioned using a vibratome (Leica VT1000). Extracellular recordings were acquired in voltage-clamp mode at near physiological temperature (34.5 ± 1 °C) using a dual-channel heat controller (Model TC-344B, Warner Instruments) and constantly perfused with carbogen-bubbled extracellular solution at a rate of 3 ml per min. Cells were visualized on an upright microscope (Leica) with a 40× water-immersion lens. Borosilicate glass pipettes with resistances of 1–3 MΩ were filled with extracellular solution and used for recording action-potential-associated capacitative current transients. The pipette potential was held at 0 mV and placed close to the Purkinje neuron axon hillock (soma/axon). Data were acquired at 20 kHz using a Multiclamp 700b amplifier, Digidata 1440 with pClamp10 (Molecular Devices) and filtered at 4 kHz. Each Purkinje neuron recording spanned a duration of 2 min and a total of 40 to over 100 cells were measured from each mouse. A total of 1–4 mice per genotype were used and the experimenter was blinded to the mouse genotype. Experiments were analysed using both Clampfit and Igor Program and further analysed using Microsoft Excel. Figures were made using Igor. Results are presented as mean ± s.e.m., unless indicated otherwise.

Statistical analysis. Statistical differences between selected groups evaluated by qPCR were determined by two-tailed Student's *t*-tests. Electrophysiological data were evaluated using analysis of variance (ANOVA) tests followed by post hoc tests of significance (Tukey's multiple-comparison test). Statistical comparisons of rotarod data were determined using the method of generalized estimating equations with the independent correlation option using Stata 12 (procedures xtset followed by xtgee). The independent correlation option was employed because in the three day rotarod paradigm, regressions for wild-type mice frequently have more positive correlation coefficients than SCA2 mice. Regression analyses were performed using GraphPad Prism.

Data availability. All data generated or analysed during this study are included in this published article (and its Supplementary Information).

29. Swayze, E. E. *et al.* Antisense oligonucleotides containing locked nucleic acid improve potency but cause significant hepatotoxicity in animals. *Nucleic Acids Res.* **35,** 687–700 (2007).
30. Langmead, B., Trapnell, C., Pop, M. & Salzberg, S. L. Ultrafast and memory-efficient alignment of short DNA sequences to the human genome. *Genome Biol*. **10,** R25 (2009).
31. Meera, P., Wallner, M. & Otis, T. S. Molecular basis for the high THIP/gaboxadol sensitivity of extrasynaptic $GABA_A$ receptors. *J. Neurophysiol*. **106,** 2057–2064 (2011).

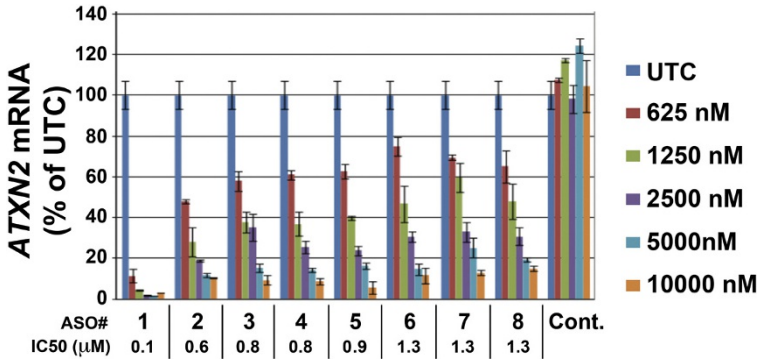

Extended Data Figure 1 | *In vitro* screen for *ATXN2* ASOs by qPCR. A total of 152 ASOs were delivered at 4.5 μM to HepG2 cells by electroporation in two 384-well plates. *ATXN2* expression was evaluated by qPCR ($n = 3$ wells per ASO). Shown is the evaluation of the eight best positive hit ASOs for half maximal inhibitory concentration (IC_{50}) determination. Values are mean ± s.d. of *ATXN2* quantity relative to total RNA. Cont., scrambled control ASO.

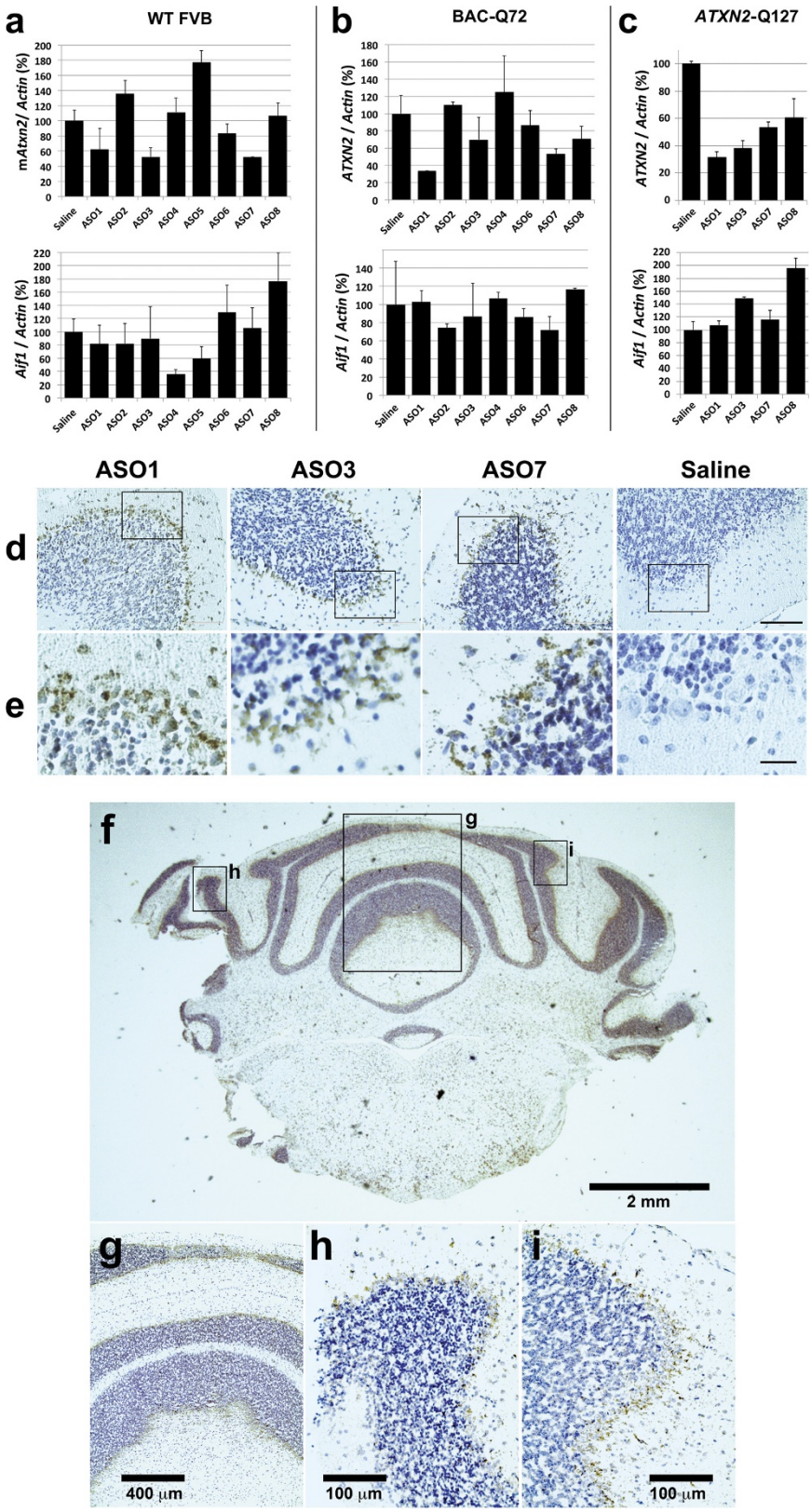

Extended Data Figure 2 | See next page for caption.

Extended Data Figure 2 | Positive hit ASOs evaluated *in vivo*. **a**–**c**, 250 μg of the indicated ASOs in a total of 7 μl was delivered by ICV injection. After 7 days treatment, the expression of mouse *Atxn2* or human *ATXN2* and *Aif1* was determined by qPCR relative to *Actb*. **a**, Wild-type FVB mice. Whereas ASO7 reduced mouse *Atxn2* the most by 50%, significant reduction of mouse *Atxn2* was not indicated by ANOVA testing for any of ASOs. ASO8 significantly elevated *Aif1* expression ($P < 0.05$). **b**, BAC-Q72 mice. *ATXN2* expression was significantly reduced by ASOs 1, 3 and 7 compared to saline ($P < 0.001$, 0.01 and 0.01, respectively). Elevations of *Aif1* was not observed compared to saline-treated mice. **c**, ATXN2-Q127 mice. Compared to saline treated mice, ASOs 1, 3, 7 and 8 all significantly lowered *ATXN2* expression by 40% or greater ($P < 0.001$), whereas ASOs 3 and 8 increased *Aif1* expression ($P < 0.001$). Values are mean ± s.d. relative to those determined from normal saline-treated mice. Statistical tests were ANOVA followed by the Bonferroni correction. Technical replication was inserted by employing qPCR with triplicate determinations, and biological replication was made by evaluating multiple mice and/or mouse lines. The number of mice (left-to-right in each chart) was as follows: **a**, $n = 2, 2, 2, 3, 2, 2, 2, 2, 1$; **b**, $n = 2, 1, 1, 2, 2, 2, 1, 2$; **c**, $n = 2, 3, 1, 1, 1$. **d**, **e**, ASOs localized to the cerebellar Purkinje cell layer of treated mice. Mice were treated by ICV injection into the right lateral ventricle of the indicated lead ASOs for 7 days in BAC-Q72 mice (ASO3 and ASO7 used at 250 μg) or 10 weeks in ATXN2-Q127 mice (ASO1 used at 200 μg). ASOs were localized in paraffin embedded sections by immunohistochemical peroxidase staining using an anti-ASO antibody. Saline, ATXN2-Q127 mice treated by ICV injection of 7 μl saline for 10 weeks. **d**, 10× objective. **e**, 3× digital zoom of a region of the Purkinje cell layer in the corresponding 10× image, indicated by the box. Scale bars, 100 μm (**d**), 25 μm (**e**). **f**–**i**, Distribution of ASO7 in the cerebellum. **f**, ASO7 was distributed in Purkinje cell layers throughout the cerebellum (2× objective). **g**–**i**, Higher power images for regions indicated in **f** showed ASO7 localization in Purkinje cells across the cerebellum: **g**, 10× objective; **h**, **i**, 40× objective.

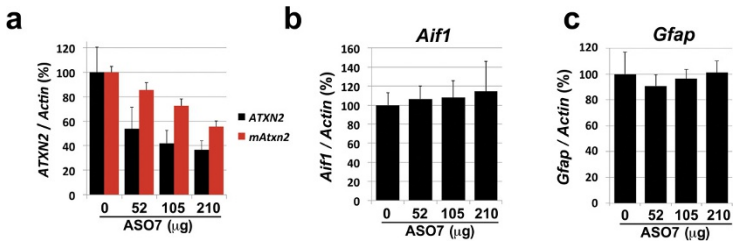

Extended Data Figure 3 | Effects of ASO7 on *ATXN2* expression *in vivo* by dose and time. a–c, Dose response for ASO7 on *ATXN2* expression in BAC-Q72 mice treated with ASO7 by ICV injection for 14 days. **a**, Expression of cerebellar human *ATXN2* and mouse *Atxn2* determined by qPCR. The 210 μM dose reduced *ATXN2* by 63.2% ($P < 0.01$) and mouse *Atxn2* by 44.5% ($P < 0.001$) compared to the 0 μM dose. The statistical test used was ANOVA followed by the Bonferroni correction. **b**, Cerebellar *Aif1* expression determined by qPCR demonstrated that *Aif1* levels were not significantly altered by ASO7 treatment. **c**, Cerebellar *Gfap* expression determined by qPCR demonstrated that *Gfap* levels were not significantly altered by ASO7 treatment. **a–c**, The replicate number of mice for the saline, 52 μg, 105 μg and 210 μg treatments was 3, 2, 3 and 3, respectively, and the values indicated are mean ± s.d. The experiment was performed once.

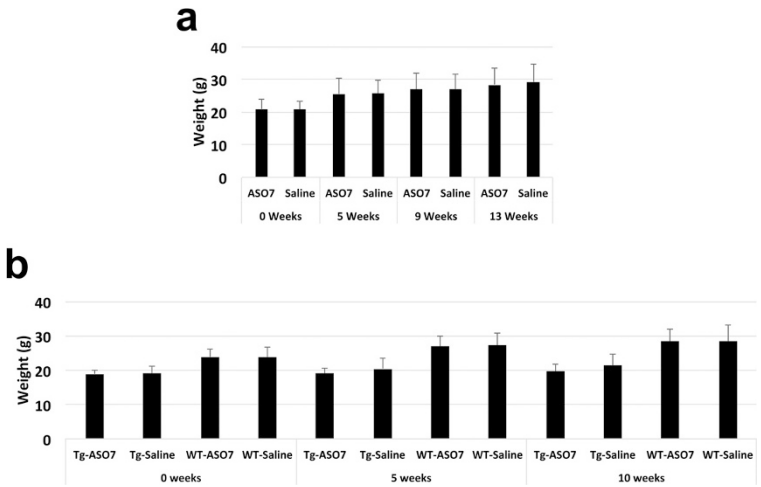

Extended Data Figure 4 | Weights of mice before and after rotarod testing. a, Rotarod test of ATXN2-Q127 mice treated with a single ICV dose of 210 μg ASO7. **b**, Rotarod test of BAC-Q72 mice treated with a single ICV dose of 175 μg ASO7. Weeks of ASO treatments are indicated on the *x* axes. Mouse weights were unaffected by ASO7 treatment. Significant differences between weights of BAC-Q72 mice compared to wild-type littermates were observed ($P < 0.001$ for any age group, Student's *t*-test). The relevance of mouse weights on motor phenotype testing is discussed in the Supplementary Discussion.

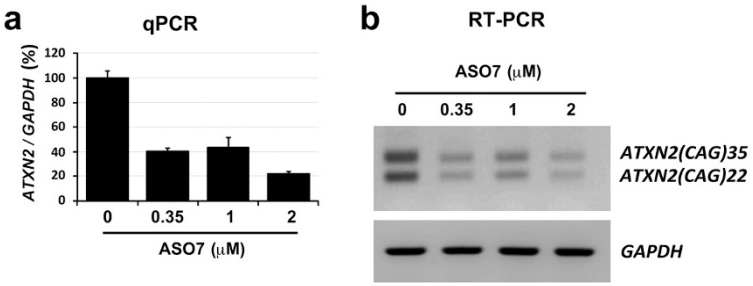

Extended Data Figure 5 | ASO7 lowered expression of wild-type and mutant *ATXN2* in cultured SCA2 patient-derived fibroblasts. a, Patient-derived SCA2(CAG35) fibroblasts were transfected with the indicated quantities of ASO7. After 72 h RNA was prepared and total *ATXN2* expression was determined by qPCR. Values are mean ± s.d. of 3 technical replicates from single cultures. *ATXN2* was reduced by 79% for the 2 μM dose compared to 0 μM ($P < 0.001$, Student's *t*-test). **b**, To determine ASO7 effect on the expression of non-mutant (CAG22) and mutant (CAG35) *ATXN2*, RT–PCR reactions were evaluated by agarose gel electrophoresis, with loading controlled for by *GAPDH*. Both **a** and **b** were replicated once yielding nearly the same result.